Journal of Electrical Engineering, Vol. 74, No. 5, 2023, pp. 382-389

sciendo
PAPERS

Thermal-magnetic performance analysis for smart fluid dampers

Antonino Caracciolo[1], Samuele Ollio[1], Alessio Pizzi[1], Leonardo Romeo[1], Antonio Enrico Serranò[1], Giuseppe Vasily Tringali[1], Antonino Greco[1], Mario Versaci[2,*]

Over the years, the Italian Government has taken significant strides in promoting road safety awareness among the students in high schools to create an awareness of prevention and a consciousness of road safety in the student population. In this context, an agreement was signed between the DICEAM Department of the "Mediterranea" University of Reggio Calabria (Italy) and the "Euclide" Higher Education Institute Bova Marina (Italy) to combine road safety with research science in the Science, Technology, Engineering, and Mathematics (STEM) area. With the primary aim of "knowing in order to act", the students focused on the multi-physics design of magnetorheological fluid dampers as high-performance devices (simple to design and requiring reduced maintenance) for vehicle suspensions, especially class B vehicles. By combining road safety considerations with multi-physics scientific disciplines, the project seeks to emphasize the importance of prevention and knowledge-based action. The study explores the use of magnetorheological fluid dampers, powered by electric current and magnetic induction distribution with thermal loads, to provide appropriate yield stress for developing damping action with repercussions on the quality of road safety. The paper delves into the basic principles of FEM (Finite Element Method) techniques for analyzing an MR damper from both magnetostatic (the main cause generating the damping effect) and thermal perspectives (thermal effects are strongly influenced by environmental conditions). The analysis of an asymmetrical device, where the damping action relies on an MR fluid strip, reveals the significant influence of magnetic and thermal stresses on the magnetization of individual particles and the overall viscosity of the MR fluid.

1 Introduction

In recent years, the Ministry of Education and Merit (MIUR) of the Italian Government has been involved in road safety education projects within schools. These initiatives utilize innovative methodologies for the involvement of student populations in prevention and training interventions to promote road safety culture, prevention and knowledge-based action (for example, respect for traffic regulations), and education for sustainable mobility among students [1, 2]. The paper highlights the emerging awareness in scientific schools of the potential synergy between road safety and scientific research in the STEM domain (Science, Technology, Engineering, and Mathematics), particularly in the automotive industry [3-5]. But in order to act, it is necessary to have a comprehensive understanding of the devices mounted on motor vehicles that directly impact road safety, including brakes and/or dampers [6-8]. While brakes have a well-established scientific-technological substrate, dampers, which are installed on vehicles to absorb and dampen impulsive shocks and reduce suspension oscillations, present intriguing open research challenges [9, 10]. In light of this, a Memorandum of Understanding was initiated between the "Euclide" High Education Institute of Bova Marina (Italy) and the DICEAM Department of the "Mediterranea" University of Reggio Calabria (Italy) to develop a path way aimed at engaging the high school student population in scientific research within the STEM area, specifically focusing on safety dampers for the automotive industry. Presently, the automotive industry offers a wide range of dampers, including hydraulic [11], magnetic effect [12], hysteretic modality [13], pneumatic, and friction [14], with well-established performance and criticalities limiting its production and diffusion. During car usage, mechanical vibrations arising from the transmission of oscillating energy can either be useful or harmful and/or destructive, necessitating cancellation or, at the very least, dampening to achieve high levels of comfort [15]. Recently, specific uses of Magnetorheological Fluids (MR) have been introduced in semi-active dampers as regulators of the damping coefficient during the stroke of the interacting piston, enabling real-time adjustments [16] through the use of external magnetic fields. These adjustments ensure instantaneous damping control based on the road surface conditions and the driver's requests, reducing vehicle movements and guaranteeing better handling and enhanced road holding with optimal wheel grip in all conditions [17]. As a result, driving becomes more enjoyable and safer due to reduced roll and enhanced control over sensitive operations such as acceleration, braking, and changes of direction.

[1]Istituto di Istruzione Superiore "Euclide", Contrada Monoscalco, I-89035 Bova Marina, Italy
[2]DICEAM Department, "Mediterranea" University, Via Graziella Feo di Vito, I-89122 Reggio Calabria, Italy
* mario.versaci@unirc.it

https://doi.org/10.2478/jee-2023-0046, Print (till 2015) ISSN 1335-3632, On-line ISSN 1339-309X

The capability of the fluid within the dampers to vary its rheological-dynamic characteristics in response to an external magnetic field, denoted as **H** and controlled by electronic devices, is key to achieving these benefits. When subjected to H, the particles suspended in the fluid promptly align themselves in chains with high mechanical resistance, effectively transforming the fluid into a material with rheological characteristics akin to extremely hard plastic [18, 19]. When the influence of **H** ceases, the particle chains instantaneously disintegrate, restoring the material to its initial rheological-dynamic properties. Even though the scientific-technological development of MR fluid dampers has advanced to a stage where high-performance MR fluid dampers can be easily produced on a large scale with minimal maintenance interventions, there remains a necessity to develop physical-mathematical models that locally and exhaustively describe the behavior of the device. These models should correspond to computationally simpler experimental counterparts, especially under specific operating conditions, enabling understanding, analysis, and prediction of the operational performance during the design phase. Obviously, the application of a greater external magnetic field strength (**H)** results in a higher induction field **B** in the coil, leading to an increase in mechanical stress, τ, until it reaches the yield stress, τ_0, giving the MR fluid a viscosity comparable to that of highly resistant plastics [20]. Experimental models typically exhibit an additive structure with weighted components, encompassing both elastic and viscoplastic contributions. The weights are formulated such that the viscoplastic components become prominent as τ approaches τ_0. Furthermore, several fundamental questions persist, both in theoretical and experimental contexts. These range from the modeling of the relationship between **H** (and therefore the electric current, *I*, generating **H**) and τ_0 (maximum permissible mechanical stress beyond which the MR fluid transitions from an extremely hard plastic to a fluid, even when $|\mathbf{H}| \neq 0$; to the physical-mathematical modeling of magneto-thermal analyses. The latter is crucial for evaluating potential overloads during the device design phase, along with assessing the influence of the absolute temperature, *T*, on the rheological properties of the MR fluid. It is worth noting that many experimental models, while computationally efficient, lack the level of detail provided by theoretical models, albeit at significantly higher computational costs. Recent developments have uncovered qualitative equivalences between theoretical models and experimental evidence. However, these equivalences have not yet fully elucidated the relationship between τ_0 and **H**, let alone the distribution of **H** (and consequently **B**) and *T* within the device. Such insights are crucial for identifying magnetic and/or thermal load-related challenges. In this paper, the project participants have venture into the analysis of a significant MR damper using Finite Element Method (FEM) techniques for the first time. This particular damper relies on a strip of MR fluid solicited by increasing *I* and circulating in the coil, producing the distribution of **B** in order to highlight potential hazardous boundary layers that could hinder the proper functioning of the device. Finally, given that *T* exerts a global influence on device performance (especially considering that the external environmental temperatures can vary significantly depending on the latitudes in which the vehicle operates), the distributions of *T* have been obtained to highlight any thermal loads compromising the correct damper operation.

The subsequent sections of the paper are structured as follows: Sections 2 and 3 propose some basic backgrounds in magnetostatics and thermostatics useful for the physical-mathematical formulation of the challenge. Section 4 presents a detailed description of the geometry of the MR fluid damper under study. Sections 5 and 6 delve into the magneto-thermo-static analysis of the device. Finally, some conclusions and future perspectives are drawn.

2 Some backgrounds for magnetostatics

Scholars approached the challenge under study by delving into Maxwell's equations for magnetostatics, which are well-recognized and take the form [21]

$$\begin{cases} \nabla \cdot \mathbf{B} = 0 \\ \nabla \times \mathbf{B} = \mu_0 \mathbf{J} \\ \mathbf{B} = \mu_0 \mathbf{H} \end{cases} \tag{1}$$

where **J** represents the electrical current density while μ_0 is the magnetic permeability of the free space; moreover, when $\mathbf{J} = 0$, **B** is solenoidal. With these premises, it is possible to consider a vector potential, **A**, in order that $\mathbf{B} = \nabla \times \mathbf{A}$ **(**although, here, the uniqueness of **B** is not ensured). Particularly,

$$\mathbf{B} = \nabla \times \mathbf{A} = \nabla \times (\mathbf{A} + \nabla f) = \nabla \times \mathbf{A} \tag{2}$$

because $\nabla \times \nabla f = 0$ since *f* can be any. However, if **J** is defined and the magnetic permeability of the material can be considered invariant with the variation of the magnetic induction, it becomes feasible to employ Biot-Savart type integral formulations. Those formulations are familiar from the basic physics courses and facilitate the modelling of the relationship between *I* and **B** [22]**.** Naturally, when dealing with simple geometries, the integral can be readily solved. For more complex geometries, the integral can be computed for each section. Finally, for the more complex geometries, the most performing technique of numerical integration would solve the challenge. Prudent consideration must be given to boundary conditions; particularly the continuity of the normal component of **B** when transitioning between materials (transit from the metal parts to the fluid MR strip). Concerning the field **H**, the ratio of the normal components strongly depends on

the magnetic permeabilities of the material involved (with **J**, the tangential components of **H** exhibit discontinuity), as known from basic physics courses, [23]. Equations (1), with suitable expedients, are sufficient to describe the magnetic-static behavior of the MR damper under study.

3 Some backgrounds for thermostatics

Indicating by $\mathbf{v} \in \mathbb{R}^3$ the vector position and by t the time variable, the flow of heat, $\mathbf{q}(\mathbf{v}, t)$, in a MR fluid can be formulated by the Fourier's law

$$\mathbf{q}(\mathbf{v}, t) = -k(\mathbf{v})\nabla T(\mathbf{v}, t) \tag{3}$$

where $T(\mathbf{v}, t)$ represents the absolute temperature and $k(\mathbf{v})$ is a coefficient taking into account the thermal peculiarities of the materials in which the heat flows. However, in homogeneous materials, k can be assumed to be independent of **v**. In such cases, the parabolic heat equation can be written as follows

$$\frac{\partial T(\mathbf{v}, t)}{\partial t} = D\,\Delta T(\mathbf{v}, t) + g(\mathbf{v}, t) \tag{4}$$

where $D > 0$ is the real diffusion coefficient while $g(\mathbf{v}, t)$ considers any external heat sources. Since (4) is an evolutionary dynamic equation, it requires both initial and boundary conditions. Particularly, if V is the domain and ∂V is its border, it is pertinent to consider the following Dirichlet boundary condition (referred to the temperature)

$$T(\mathbf{v}, t) = T_q, \quad \mathbf{v} \in \partial V \tag{5}$$

Even if Neumann boundary conditions (since they are referred to the heat flux across the edges)

$$k\nabla T(\mathbf{v}, t) \cdot \mathbf{n} = q, \quad \mathbf{v} \in \partial V. \tag{6}$$

could be exploited. Concerning the initial condition, it can be written as follows:

$$T(\mathbf{v}, 0) = h(\mathbf{v}), \ \mathbf{v} \in \partial V \tag{7}$$

while, no conditions are assigned at the final time, $\bar{t}$, because all conditions are assigned just on the parabolic, $\partial_P Q_T$, where Q_T is the cylinder constituted by

$$[(V(\cup \partial V) \times \{t = 0\}] \cup \partial V \times (0, \bar{t}\,]. \tag{8}$$

Moreover, indicating by h and k_1 the thermal conductivity and the heat transfer coefficient, respectively, the law of cooling becomes:

$$h\nabla T(\mathbf{v}, t) \cdot \mathbf{n} = -k_1\big(T(\mathbf{v}.t) - T_q\big), \quad \mathbf{v} \in \partial V. \tag{9}$$

Obviously, in our case,

$$T = T(\mathbf{v}), \quad g = g(\mathbf{v}) \tag{10}$$

so that Eqn. (4) becomes

$$D\,\Delta T(\mathbf{v}) + g(\mathbf{v}) = 0 \tag{11}$$

Finally, without external heat source (i.e., $g(\mathbf{v}) = 0$), the thermostatic model becomes:

$$\begin{cases} \Delta T(\mathbf{v}) = 0 & \mathbf{v} \in V \\ T(\mathbf{v}) = T_q & \mathbf{v} \in \partial V. \end{cases} \tag{12}$$

It is evident that before solving (12), it is necessary to establish whether it admits a unique solution. As per a well-known theorem [24], since the external source is zero (and, therefore, continuous together with its first derivative), it follows that (1) admits a unique solution that is sufficiently regular exhibiting high spatial gradients and, therefore, potentially dangerous boundary layers in some areas of the device (as, moreover, predicted by the maximum theorems [25]). Furthermore, the solution is easily obtainable when the device consists of simple geometry while numerical approaches are needed for complex geometries. In all cases, in order to circumvent spurious solutions (i.e., numerical solutions that do not satisfy any condition of existence and uniqueness of the analytic solution) it is imperative to possess algebraic conditions (preferably in the form of an increase) ensuring existence, uniqueness and possibly regularity of the solution for the equation (9) [25].

4 The device under study: MR fluid damper for automotive applications

The damper under study, depicted in Fig. 1, consists of a steel piston (with a Young's modulus equal to 2.1×10^{11} Pa and a Poisson's coefficient equal to 0.31) with a radius, *R*, which contains the housing of the coils, which, upon passage of *I*, generate **H**. The piston-coil coupling is in turn contained in a steel cylinder with a thickness, represented as *t*, equal to 9 mm with an air gap of 11 mm in which the strip of MR fluid is located. Additionally, the distance from the piston rod to the inner edge of the spool, designated as *H*, measures 8 mm. Finally, the piston is configured to contain the coil (length *l* equal to 23 mm) inside it, with post length *L* equal to 24 mm. Regarding the MR fluid, the focus is on the MRF-132AD product manufactured by the Lord Corporation, as it is the most commonly used for dampers in the automotive industry.

The device, as described here, represents the schematization of real devices already in use in the automotive industry of high-performance cars. It is worth noting that the device under study has been extensively studied in [26] using a very detailed theoretical approach, based on thermodynamic with tensor internal variable and constitutive equations, but suffering from high computational complexity and therefore not suitable for any real-time applications.

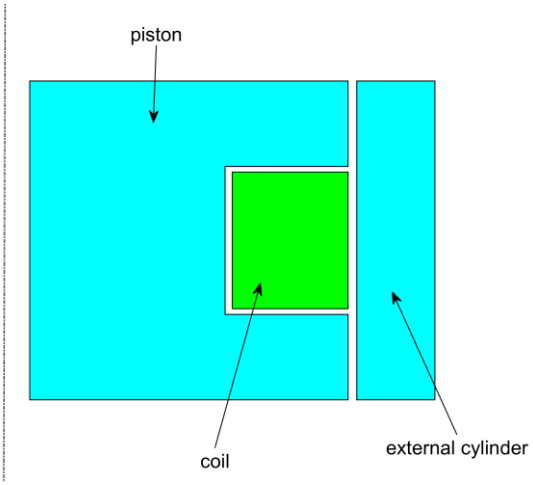

Fig. 1. 1D Schematization of the MR fluid damper under study: MR fluid strip is located in the air gap separating the piston that contains the external cylinder (the vertical line on the left represents the device axis of symmetry).

5 On the magnetostatic analysis of the device

The analytical model, given the geometry, is difficult to solve explicitly, so we rely on FEM numerical procedures. Particularly, we used the ANSYS ToolBox and, especially, its module 13, which is capable of solving magneto-thermo-static problems. As known, if *N* is the number of windings of the coil having a certain length, *L*, and a section, *A*, the amplitude of the current density, **J**, can be calculated as

$$|\boldsymbol{J}| = \frac{NI}{AL} \tag{13}$$

where *I* is the current flowing in the coil. We observe that in commercial vehicles, the battery usually supplies 12 V while the loads vary according to the running conditions of the vehicle.

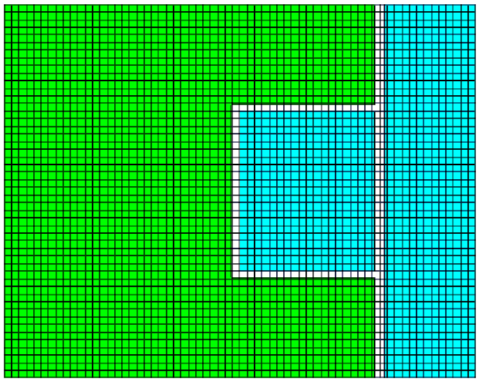

Fig. 2. Mesh for the FEM approach

Table 1.
$|\mathbf{B}|_{\min}$ and $|\mathbf{B}|_{\max}$ as *I* increases

I (Ampere)	$\lvert\mathbf{B}\rvert_{\mathrm{MIN}}$ (Tesla)	$\lvert\mathbf{B}\rvert_{\mathrm{MAX}}$ (Tesla)
2	6.94×10^{-5}	0.892
3	1.43×10^{-4}	0.914
4	1.49×10^{-4}	0.966
5	1.86×10^{-4}	0.999
6	2.19×10^{-4}	1.04
7	2.61×10^{-4}	1.19
8	2.94×10^{-4}	1.23
9	3.26×10^{-3}	1.26
10	3.49×10^{-3}	1.30
11	3.97×10^{-2}	1.38
12	4.65×10^{-2}	1.40

Since *I* strongly depends on the resistive loads, it appears imperative to study the behavior of the damper under different load conditions and, therefore, as *I* vary. It follows that by increasing *I*, |**B**| increases, resulting in increased viscosity and τ of the MR fluid. So, to make the $\tau - |\mathbf{B}|$ link, we will exploit a polynomial expression as [27]

$$\tau(|\mathbf{B}|) = \sum_{i=0}^{3} a_i |\mathbf{B}|^{4-i}, \qquad a_i \in \mathbb{R}^+ \tag{14}$$

able to achieve, as *I* increase, the corresponding $|\mathbf{B}_{\max}|$ from which to get τ_0. However, as can be seen from Fig. 1, the geometry of the MR damper is delimited by edges parallel to the lines of force of **B,** allowing the construction of a regular mesh whose finite elements are quadrangular in shape [24]. With this premise, we subdivide the domain *V* into *m* sub-regions, S_r, (i.e., cylinder coil, ...) juxtaposed to each other (i.e., $S_r \cap S_{r'} = \emptyset$ with $r \neq r'$ such that their union, $\bigcup_{r=1}^{m} S_r$, entirely covers *V*. Each sub-region is subdivided into m_T quadrangular finite elements for which *V* is representable as $\bigcup_{s=1}^{m_T} T_s$, such that $T_s \cap T_{s'} = \emptyset$, with $s \neq s'$. It is worth noting that the mesh thus constructed is well-posed since, $\forall s \neq s'$, it is easy to verify that $T_s \cup T_{s'}$ is either empty or consists of exactly one node or one edge and each finite element is characterized by zero measure. Moreover, the quality of the mesh has been verified by well-established parameters, such as the index of skewness (measuring the deviation of a cell from an ideal cell) and the aspect ratio calculations (measures of the stretching of a cell). The mesh, made up of 6018 nodes forming 4824 finite elements delimited by 3874 surface elements, has been achieved through a Delaunay procedure for non-convex domains (such as the domain under study), obtaining a regular distribution of finite elements by selecting a set of edges constructed in such a way that the mesh associates the afore-mentioned edges to a pre-established set of finite elements (Fig. 2). Particularly, the elements of the mesh

have been structured in such a way that the sphere circumscribed by each finite element has no vertices inside it.

Once the mesh has been built, I has been circulated in the coil so that the vector potential **A** is set to zero; then, since locally the mechanical stress depends on τ (which, in turn, depends on $|\mathbf{B}|$) for each point of the domain, the norm of the difference of $|\mathbf{B}|$ in two successive iterations

$$||\mathbf{B}|^{j+1} - |\mathbf{B}|^{j}| \tag{15}$$

has been evaluated so that the procedure stops when its variation is null (or, in any case, below a certain small threshold, as desired). However, it must be taken into account that $|\mathbf{B}|$ increases as I increase. Subsequently, it becomes meaningful to compute $|\mathbf{B}|$ whose electric current values ranging from 2 A to 12 A, as currently used in the design practice of MR dampers for the automotive industry. Such values of $|\mathbf{B}|$ are displayed in Table 1, revealing a maximum value of $|\mathbf{B}|$ at approximately 1.4 T. This value notably remains well below the saturation value of the MR fluid considered (confirming the initial hypothesis consisting of neglecting the presence of any housing cover and neglecting the eddy currents). The magnetostatic analysis carried out showed that, when I is maximum, the most magnetically stressed area is the strip of MR fluid; however, as already highlighted, **B** is strongly below the saturation value, therefore the optimal performance of the damper is ensured.

To specify $\tau(|\mathbf{B}|)$, the conventional Bingham model cannot be used as we do not know τ_0. Then, we adapt (14) to the specific case of the type of MR fluid used (Lord MRF-132AD fluid) by setting a_i as follows [27]

$$a_0 = 6.5, \qquad a_1 = -26.1,$$
$$a_2 = 26.9, \qquad a_3 = -0.59 \tag{16}$$

so that, by replacing $|\mathbf{B}_{\max}|$ for $|\mathbf{B}|$, (14) gives the required link. As shown in Table 2 and in Fig. 3, the studied damper, offers very good mechanical resistance since the maximum current circulates in the coil, $\tau_0 = 146$ kPa, which is also confirmed by the fact that the mechanical force in the damper, calculated as described in [27] exceeds 10 kN when the current circulating the coil is the maximum allowed.

Finally, since the device operates in shear mode (i.e., the surfaces have a relative motion with respect to each other in which the MR fluid operates), the force created consists of two independent viscous components:

$$|\mathbf{F}| = \left[\frac{S \cdot A \cdot \eta}{g}\right] + A \cdot \tau_{mr} \tag{17}$$

where S represents the relative speed of the surfaces, A is the surface area, g is the fluid gap, η is the viscosity, and τ_{mr} is the yield stress variable in response to an applied magnetic field. The trend of (17) is such that, when the piston speed is the maximum allowed, it develops a force of 10.14 kN.

Table 2.
τ_0 as I increases

I (Ampere)	τ_0 (kPa)
2	41.0
3	44.7
4	50.5
5	55.0
6	57.5
7	59.9
8	73.9
9	78.5
10	84.3
11	125
12	146

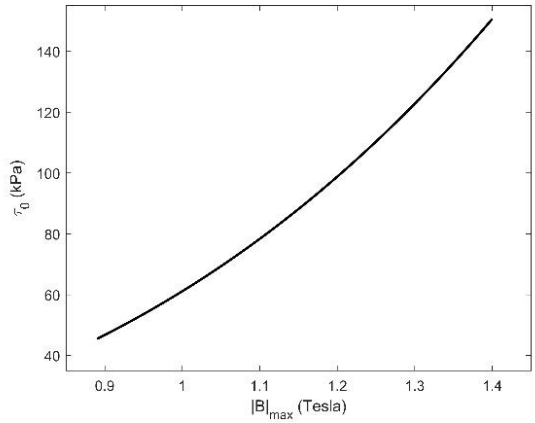

Fig. 3. Trend of the yield stress as the current circulating in the coil increases

6 On the thermostatic analysis of the device under study

Starting from the assumption that in MR dampers, the heat propagates only by conduction (since convection and radiation are practically nil), Eqn. (12) has been solved numerically without an external heat source using a mesh (constructed with the same procedure used in the magneto-static analysis) but less dense than in the previous case (496 finite elements, 394 surface elements, and 731 nodes) as the heat transmission is supposed to be in a static regime. The generated heat maps have revealed distinctly differentiated $T(\mathbf{v})$ distributions, with high thermal loads in correspondence with the MR fluid strip. However, acknowledging that the damper is potentially utilized on vehicles operating at different latitudes, the heat maps were as varied as T_q possible. Particularly, for $T_q < 263$ K, the MR fluid strip is subjected to a limited thermal load: insufficient heat is

generated within the MR fluid to facilitate substantial heat transfer to other segments of the device. However, even if T_q increases, the maximum detectable absolute temperature undergoes minor fluctuations in comparison to its minimum value, which increases significantly.

Consequently, $T(\mathbf{v})$ in the MR fluid levels remains (albeit with slight fluctuations), while the other sections of the device $T(\mathbf{v})$ exhibit comparatively higher values, albeit without undergoing substantial changes. The scenario changes when T_q exceeds 323 K (while remaining below 413 K). In this case, the absolute temperature within the piston exhibits negligible fluctuations, yet substantial variations are observed within the housing, causing noteworthy shifts in the viscosity, η, of the MR fluid. Specifically, based on [27], the relationship is expressed as

$$\eta\big(T(\mathbf{v})\big) = 0.2 - 11 \times 10^{-4}\, T(\mathbf{v}) \tag{18}$$

which shows that increases in $T(\mathbf{v})$ linearly affect decreases in η which reaches its maximum value at absolute zero temperature.

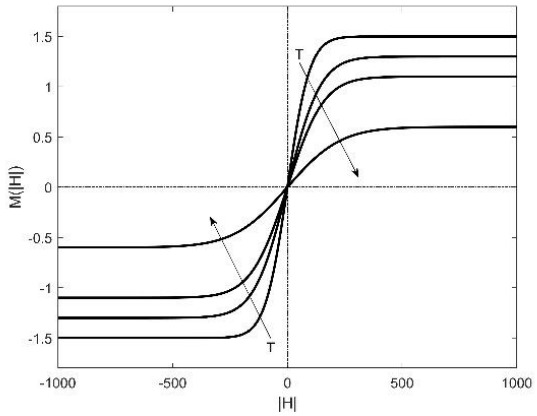

Fig. 4. Trend of $M(|\mathbf{H}|)$ as T increases

Temperature, in addition to globally influencing the MR fluid (change in η), also influences the magnetization, $M(|\mathbf{H}|)$, of the particles suspended in the MR fluid. Particularly, by [27],

$$\begin{cases} M(|\mathbf{H}|) = M_s \left[\coth\left(\dfrac{\mu|\mathbf{H}|}{k_B T}\right) - \left(\dfrac{k_B T}{\mu|\mathbf{H}|}\right)\right] \\ M_S = 8.1661\ \mathrm{e}^{\frac{3T}{1000}} \end{cases} \tag{19}$$

where M_s is the saturation magnetization and k_B is Boltzmann's constant. Then, when $|\mathbf{B}_{\max}| = 1.4$ T, through (18), $|\mathbf{H}_{\max}|$ is obtained, and by increasing T_q from 243 K to 413 K, it is evident that $M(|\mathbf{H}|)$ decreases almost linearly when the temperature is low, while the decrease in temperature causes a greater variation of $M(|\mathbf{H}|)$. However, at low temperatures, $M(|\mathbf{H}|)$ shows a trend parallel to the increase of $|\mathbf{H}|$ which also occurs at high temperatures but with significant values of $|\mathbf{H}|$ (see Fig. 4). We point out that the temperature also influences the first magnetization curve, which flattens considerably, highlighting extremely low saturation values.

7 Conclusions and perspectives

In this paper, we have presented a FEM magneto-thermo-static analysis of an automotive industry damper wherein the damping mechanism relies on a strip of commercially available MR fluid characterized by specific rheological properties. Beginning with a physical-mathematical point of view using a magneto-static approach with Dirichlet boundary conditions, important aspects of heat conduction within the device have been formalized using Fourier's parabolic formulation. The geometry of the MR damper was defined and implemented into the ANSYS Toolbox (which allows formulations of multi-physics problems). By configuring the rheological parameters of the MR fluid, a FEM magnetostatic analysis of the device was conducted, revealing the correlation between increased electric current within the coil and elevated values of magnetic induction. These values, though distant from saturation, establish a link with yield strength through polynomial formulations widely used in experimental and industrial practice. The analysis shows that the strip of MR fluid is the most magnetically stressed, also highlighting that the maximum induction causes an increase in the yield strength of the MR fluid, showing a considerable mechanical strength. Furthermore, given that past experience has highlighted changes in rheological behavior as the external temperature of the device varies, thermal maps have been made for certain values of external temperature simulating even extreme environmental conditions to highlight the temperature boundary layers. Furthermore, a study of the influence of temperature both on the fluid as a whole (the influence of temperature on the viscosity of the MR fluid, which increases with decreasing temperature) and on the magnetization of the particles was conducted. This has made it possible to highlight strong reductions in residual magnetization with consequent extremely compressed hysteresis cycles with evident reductions in any losses (See Figure 4). Finally, it is worth noting how the decrease in coercivity (due to the flattening of the hysteresis loop) is caused by the increase in temperature. This temperature-induced increase accelerates atomic activity, consequently perturbing the magnetic moments of the particles of the MR fluid.

While the obtained results exhibit promising rheological characteristics, they should be regarded as an initial step. Despite the encouraging outcomes achieved, there exists an opportunity to make additional efforts to take into account non-linearities in the thermal conductivity – a factor inherently dependent on temperature. Moreover, the advocated approach should

incorporate considerations for the non-instantaneous distribution of temperature and acknowledge that the laser beam, interacting with localized material areas, may introduce microstructural disturbances. Then, in the future, there is a call for investigations employing more realistic 3D geometries and encompassing a broader array of commercial MR fluids exploiting the results achieved here in order to highlight any progress of critical issues. Furthermore, embarking on a more comprehensive magneto-thermostatic study is advisable. Such a study could address delayed heat flow and temperature distribution while placing heightened emphasis on the interrelationship between the yield stress and the induction field. This interplay, as delineated earlier through the Biot-Savart type formulations, establishes a connection between the electric current circulating in the coil and the yield stress.

References

[1] M. Coltelli, A. Dispenza and S. Cimarra, Sulla strada in sicurezza, Roma, Italy: Il Capitello, 2020.

[2] M. Haghani, A. Behnood, V. Dixit and O. Oviedo-Trespalacios, "Road safety research in the context of low- and middle-income countries: macro-scale literature analysis, trends, knowledge gaps and challenges", *Safety Science*, vol. 146, pp. 105513-105537, 2022.

[3] M. M. Rahman, M. K. Islam, A. Al-Shayeb and M. Arifuzzaman, "Towards sustainable road safety in saudi arabia: exploring traffic accident causes associated with driving behavior using a bayesian belief network", *Sustainability*, vol. 14, no. 10, pp. 6315-6334, 2022.

[4] M. Guzek, K. I. Jurecki and W. Wach, "Vehicle and traffic safety", *Energies*, vol. 15, no. 13, pp. 4573-4596, 2022.

[5] G. A. Henok, "Safety policy in Addis Abeba: a vision zero perspective", *Sustainability*, vol. 14, n. 9, pp. 5318-5336, 2022.

[6] D. Piromalis and A. Kantaros, "Digital twins in the automotive industry: the road toward physical-digital convergence", *Applied System Innovation*, vol. 5, pp. 65-79, 2022.

[7] H. T. Cheng, H. Shan and W. Zhuang, "Infotainment and road safety service support in vehicular networking: from a communication perspective", *Mechanical Systems and Signal Processing*, vol. 25, no. 6, pp. 2020-2038, 2021.

[8] Z. Lyu and C. Wang, "Predictive shift strategy of dual-clutch transmission for driving safety on the curve road combined with an electronic map", *SAE International Journal of Vehicle Dynamics, Stability and NVH-V132-10EJ*, vol. 12, no. 3, pp. 3-21, 2022.

[9] C. Itu, A. Toderita, L. V. Melnic and S. Vlase, "Effect of seat belts amd shock adsorbers on the safety of racingrscar driven", *Mathematics*, vol. 10, pp. 3593-3611, 2022.

[10] Y. Zou, F. Xue, K. Shi, X. He, Y. Han, Q. Liu and L. Li, "Analysis of the effects of wind barrier on driving safety and comfort of vehicles of long-span bridges under crosswinds", *Mathematics*, vol. 42, pp. 367-385, 2022.

[11] S. Adhikari and J. Woodhouse, "Identification of damping: Part 1, viscous damping", *Journal Sound Vibrations*, vol. 243, pp. 43-61, 2011.

[12] Y. Furuichi and T. Tagawa, "Numerical study of the magnetic damping effect on the sloshing of liquid oxygen in a propellant tank", *Fluids*, vol. 5, pp. 88-99, 2020.

[13] F. Tatsuoka, T. Iwasaki and Y. Takagi, "Hysteretic damping of sands under cyclic loading and its relation to shear modulus", *Soils Found*, vol. 18, pp. 25-40, 2005.

[14] C. Pierre, A. A. Ferri and E. H. Dowell, "Multi-harmonic analysis of dry friction damped systems using an incremental harmonic balance method", *Journal of Applied Mechanics*, vol. 52, pp. 958-964, 1985.

[15] S. H. Crandall, "The role of damping and vibration", *Journal Sound Vibrations*, vol. 11, pp. 3-18, 1980.

[16] X. X. Bai, N. M. Wereley and D. Wang, "Controllability of magnetorheological shock absorber: Part I. Insights, modeling and simulation", *Smart Materials and Structures*, vol. 28, pp. 15022-15041, 2018.

[17] T. Lenkutis, D. Virzonis, A. Cerskus, A. Dzedzickis, M. Sesok and V. Bucinskas, "Automotive ferrofluidic electromagnetic system for energy harvesting and adaptive damping", *Sensors*, vol. 1195, pp. 1-29, 2022.

[18] M. Versaci and A. Palumbo, "Magnetorheological fluids: qualitative comparison between a mixture model in the extended irreversible thermodynamics framework and an Herschel-Bulkley experimental elastovisco-plastic model", *International Journal of Non-Linear Mechanics*, vol. 118, pp. 1-18, 2020.

[19] M. Versaci, A. Cutrupi and A. Palumbo, "A magneto-thermo-static study of a magneto-rheological fluid damper: a finite element analysis", I*EEE Transactions on Magnetics*, vol. 57, no. 1, pp. 1-10, 2020.

[20] P. Saramito, Complex Fluids, *Modeling and Algorithms*, Switzerland: Springer International Publishing, 2016.

[21] M. Cacciola, F. La Foresta, F. C. Morabito and M. Versaci, "Advanced use of soft computing and eddy current test to evaluate mechanical integrity of metallic plates", NDT and E International, vol. 40, no. 5, pp. 357-362, 2007.

[22] F. C. Morabito and A. Versaci, "A fuzzy neural approach to loalizing holesin conducting plates", I*EEE Transactions on Magnetics*, vol. 37, no. 5 I, pp. 3534-3537, 2001.

[23] G. Mrozynski and M. Stallein, *Electromagnetic field theory*, Wiesbaden: Springer Vieweg, 2013.

[24] A. Quarteroni, *Numerical models for differential problems*, Springer, 2015.

[25] P. Boeckh and T. Wetzel, *Heat Transfer*, Berlin Heidelberg: Springer-Verlag, 2012.

[26] K. Ozsoy and M. R. Usal, "A mathematical model for the magnetorheological materials and magneto rheological devices", *Engineering Science and Technology, an International Journal*, pp. 1143-1151, 2018.

[27] A. Hajalilou, S. A. Mazlan, K. Lavvafi and K. Shameli, *Field responsive fluids as smart matherials*, Singapore: Springer Nature, 2016.

Received 24 August 2023